Spin-polarized 3He : liquid gas equilibrium

S. Stringari, M. Barranco, A. Polls, P.J. Nacher, F. Laloë

J. Physique **48** (1987) 1337-1350 AOÛT **1987**, PAGE 1337

Classification
Physics Abstracts
67.50 — 64.70F

Spin-polarized ^{3}He : liquid gas equilibrium

S. Stringari (*), M. Barranco (+), A. Polls (+), P. J. Nacher (△) and F. Laloë (△)

(*) Dipartimento di Fisica, Università di Trento, 38050 Povo, Italy
(+) Departament d'Estructura i Constituents de la Matèria, Universitat de Barcelona, Facultat de Fisica, Diagonal 647, 08028 Barcelona, Spain
(△) Laboratoire de Physique de l'ENS, 24, rue Lhomond, 75005 Paris, France

(*Reçu le 29 janvier 1987, accepté le 8 avril 1987*)

Résumé. — Nous étudions les effets de la polarisation nucléaire M sur le diagramme d'équilibre liquide-gaz de ^{3}He, dans des situations où la pression de vapeur saturante croît ou décroît en fonction de M, et où une instabilité métamagnétique peut se produire dans le liquide. Nous donnons des prédictions numériques obtenues dans le cadre d'un modèle phénoménologique dont les paramètres sont choisis de façon à reproduire avec précision la pression de vapeur saturante et la susceptibilité magnétique du liquide ordinaire (non polarisé). Pour des températures de l'ordre de 0,5 K, on trouve dans certains cas des situations où se produisent des phénomènes intéressants, tel qu'une surpolarisation du liquide ou un plateau métamagnétique.

Abstract. — We study the effects of nuclear polarization M on the liquid-gas equilibrium phase diagram of ^{3}He, in situations where the saturating vapour pressure increases or decreases as a function of M, and where a metamagnetic instability may occur in the liquid phase. Numerical predictions are given within the frame of a phenomenological model with parameters fitted to reproduce accurately the saturating vapour pressure of the unpolarized liquid as well as its magnetic susceptibility. At temperatures of the order of 0.5 K situations are found where interesting phenomena such as liquid overpolarization and metamagnetic plateaus occur.

There is currently an active interest in phase transitions in spin-polarized ^{3}He. Several groups [1, 2] have recently obtained interesting results on the solid-liquid transition, using the polarization method proposed by Castaing and Nozières [3]. The results might indicate the existence of a metamagnetic transition (or near metamagnetic transition), as suggested by B. Castaing [4] and by K. Bedell and C. Sanchez-Castro [5]. Such a transition could also have an important effect on the superfluid properties of the liquid [6].

In the present article, we study another transition which takes place at lower pressures, the liquid-gas transition. Gaseous ^{3}He can be strongly polarized by laser optical pumping [7], but also cooled down and condensed to form liquid ^{3}He ↑ , which should allow studying the effects of the nuclear polarization on the saturating vapour pressure. These effects are non-trivial [8] : for example, the nuclear polarizations of the two phases at equilibrium can be significantly different, because particle indistinguishability effects are more important in the (denser) liquid phase than in (dilute) gas phase. Liquefaction experiments of this type are in progress at the Ecole Normale [9]. Experimental data would give access to physical quantities which depend on many body effects and are difficult to calculate, such as the change of the binding energy of the liquid under the effect of spin polarization. Moreover, they might also reveal the existence of a metamagnetic transition in the liquid phase, as we see in more detail below.

To study these problems, in the present article we use a simplified model already employed for investigating the thermodynamical properties of asymmetrical nuclear matter [10]. In a nucleus, the asymmetry (difference between the number of neutrons and protons) plays the role of spin polarization (difference between the number of spin up and spin down particles) in ^{3}He system ; asymmetrical nuclear matter occurs in several important problems in astrophysics [11]. The model is based on the use of a Skyrme interaction [12] in the framework of a mean-

field approach [13, 14]. It is also employed in a joined article [15] (hereafter referred to as BPS) on the liquid-gas transition in unpolarized ^{3}He.

1. General framework.

1.1 CROSS-OVER TEMPERATURE T^*. — In the limit of very low temperatures, the saturated (unpolarized) ^{3}He vapour is very close to an ideal gas, and its chemical potential has the simple following expression

$$\mu_G = kT[\text{Log } n\lambda^3 - \text{Log } 2] \tag{1}$$

where $\lambda = h\,(2\,\pi mkT)^{-1/2}$ is the thermal wavelength of the ^{3}He atoms, k the Boltzmann constant, T the temperature and n the number density. This chemical potential is purely entropic ; in particular, the term in Log 2 is due to spin entropy. On the other hand, at low temperatures, the chemical potential μ_L of the atoms in the liquid phase is almost pure energy and equal to E, the energy per atom ($E \simeq -2.5$ K) ; the liquid being degenerate, there is no spin entropy. Equating both μ's gives the temperature dependence of the saturating vapour pressure P for ordinary (unpolarized) ^{3}He :

$$P \simeq 2\,A\,T^{5/2} \exp(E/kT) \tag{2}$$

where A is a constant. For fully polarized ^{3}He, the saturating pressure $P\uparrow$ is given by

$$P\uparrow \simeq A\,T^{5/2} \exp(E\uparrow/kT) \tag{3}$$

where $E\uparrow$ is the (negative) energy per atom in the polarized liquid, which is expected to be smaller (in absolute value) than for unpolarized liquid [8]. In (3) there is no factor 2 because a fully polarized gas does not have any spin entropy. Therefore :

$$\frac{P\uparrow}{P} \simeq \frac{1}{2} \exp \frac{\Delta E}{kT} \tag{4}$$

with

$$\Delta E = E\uparrow - E \tag{5a}$$

There are consequently two regimes, depending on the relative values of the temperature with respect to a cross-over temperature T^* defined by :

$$kT^* = \frac{\Delta E}{\text{Log } 2}\,. \tag{5b}$$

If $T < T^*$, the energy effects dominate and as discussed in [8], the saturating vapour pressure of ^{3}He$\uparrow$ is larger than that of ^{3}He. But ([1]), if $T \gtrsim T^*$, nuclear spin entropy is important and the reverse is true ($P\uparrow < P$).

([1]) The discussion of paragraphn 3.2.1 of [8] is not correct because the factor 1/2 in equation (4) is omitted.

Actually, when $T > T^*$, the preceding equations do not necessarily apply, since they are only valid in the limit of very low temperatures. At higher temperatures, the liquid is no longer completely degenerate and acquires a spin entropy (which, in the limit of high temperatures, approaches that of the gas phase, so that the factor 1/2 in (4) comes closer to 1). Moreover, the motional entropy of the atoms in the liquid is no longer negligible. Nevertheless, the above discussion remains qualitatively valid and, in section 3, we will find situations where a cross-over temperature T^* indeed occurs, with an order of magnitude given by (5b).

1.2 CONSTRUCTION OF PHASE DIAGRAMS. — For the present discussion, which is strongly inspired by the beginning of [3], it is convenient to take as thermodynamical variables N (total number of particles), P (pressure), T (temperature) and finally M (nuclear polarization) ; M is defined as a dimensionless number ($-1 \leqslant M \leqslant +1$) by

$$\mathcal{M} = N\mu_n M \tag{6a}$$

where μ_n is the ^{3}He nuclear moment and $\mathcal{M}$ the total magnetic moment of the sample. This is a convenient choice of variables for studying (metastable) equilibrium situations where M varies very slowly in time, under the effect of nuclear relaxation (relaxation times can be of the order of minutes in the liquid phase [16], hours or even days in the gas phase [17]). An alternative choice is to replace the variable M by the effective (or « internal ») magnetic field :

$$B_{\text{eff}} = [1/N\mu_n] \frac{\partial G}{\partial M}\bigg|_{P,T} \tag{6b}$$

where G is the Gibbs free energy of the system. For what follows, it is convenient to introduce the free-energy per atom g :

$$g = G/N\,. \tag{6c}$$

At fixed temperature and pressure, the variations of g as a function of M have the form shown in figure 1a. For the gas phase, where degeneracy effects are negligible, the energy does not depend on M and all the variation of g are contained in the spin entropy term s_I :

$$k^{-1} s_I = \frac{1}{2}(1+M)\,\text{Log}\left[\frac{1}{2}(1+M)\right] + \frac{1}{2}(1-M)\,\text{Log}\left[\frac{1}{2}(1-M)\right]. \tag{7}$$

This expression replaces Log 2 in the right hand side of equation (1) for a partially polarized gas. For the liquid phase, in addition to spin and atom motion entropy, degeneracy effects introduce a M dependence of the energy U ; so, even at zero temperature,

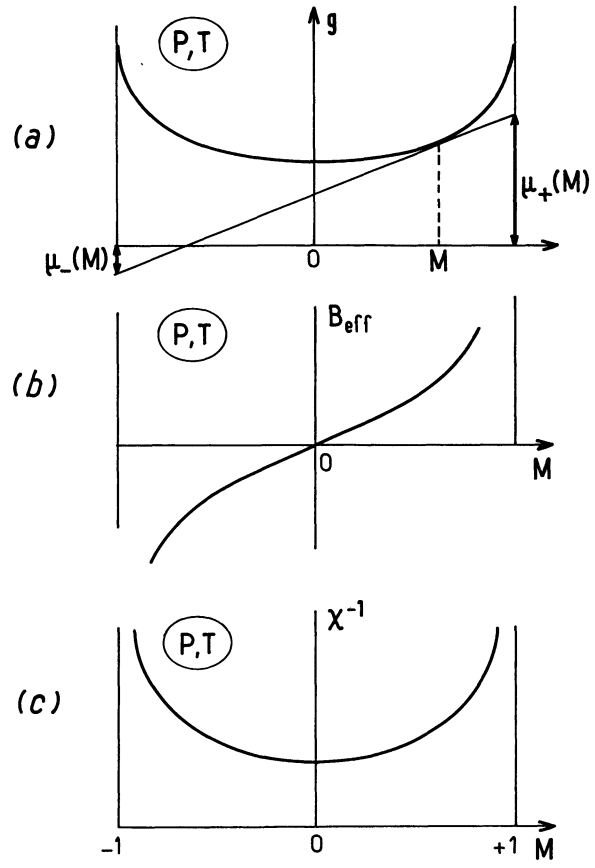

Fig. 1. — The upper curve shows the variations of the Gibbs free energy per atom g as a function of the (relative) magnetization M, at fixed pressure and temperature. A simple geometrical construction gives the chemical potentials $\mu_+ (M, P, T)$ and $\mu_- (M, P, T)$ of spin up and spin down atoms. A partial derivation of g with respect to M leads to the effective field B_{eff} which is proportional to $\mu_+ - \mu_-$, and a second derivation gives the inverse magnetic susceptibility χ^{-1}.

the curve has the convex shape in figure 1a. The same figure shows the simple geometrical construction which gives $\mu_+ (P, T)$ and $\mu_- (P, T)$, the chemical potentials of spin up and spin down atoms respectively (*). These two quantities are related by [3] :

$$\mu_+ - \mu_- = 2\,\mu_n\, B_{\text{eff}} . \qquad (8)$$

A derivation of g with respect to M (at constant P, T) gives B_{eff}, as shown in figure 1b, and a second derivation gives the inverse of the magnetic susceptibility per atom :

$$\chi^{-1} = [1/\mu_n]^2 \left.\frac{\partial^2 g}{\partial M^2}\right|_{P,T} \propto \left[\frac{\partial \mu_+}{\partial M} - \frac{\partial \mu_-}{\partial M}\right]_{P,T} . \qquad (9)$$

Now, if two phases coexist, one has to consider the two corresponding curves giving g as a function of M. When, for instance, P varies at fixed T, the curve giving g for the gas phase moves vertically by a larger amount than that of the liquid phase (because the term in Pv is larger in a dilute phase). Therefore, in some pressure range, the two curves will intersect as shown in the upper part of figure 2. A common tangent construction (convex envelope) shows that, for any magnetization M between M_1 and M_2, the system separates spontaneously into two different phases, gas and liquid in equilibrium. The geometrical construction of the equilibrium curves is shown in the lower part of the figure. Coming back to the geometrical construction of the chemical potentials in figure 1, one sees that the effective fields in the two phases, as well as the two chemical potentials, are indeed equal at equilibrium, as expected ; from now on, the common value of the two effective fields will be noted B.

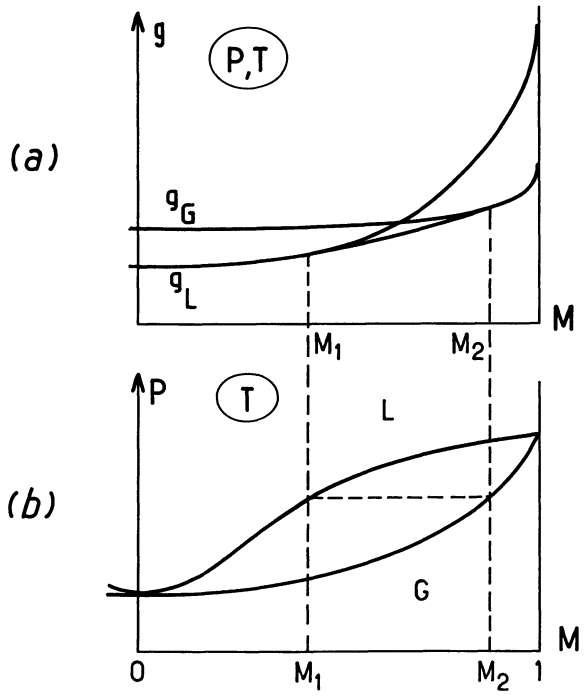

Fig. 2. — Geometrical construction of the phase equilibrium diagram between gas and liquid. Figure (a) shows the variations of the two g curves g_G for the gas, g_L for the liquid phase. The contact points of the common tangent give respectively the two magnetizations M_1 and M_2 of the liquid and gas in equilibrium. When P varies at constant T, one obtains the equilibrium diagram in figure (b).

(*) We take here the point of view where the spin up and spin down atoms are treated as two different atomic species, with two chemical potentials (which are separately equal in two phases at equilibrium). It can be shown rigorously in quantum mechanics that this point of view is completely equivalent to that where all atoms are considered identical and where antisymmetrization acts also on spin states.

1.3 ROLE OF MAGNETIC SUSCEPTIBILITIES (*). — The Gibbs-Duhem relation gives

$$\mu_n(M_L - M_G)\,dB = (v_L - v_G)\,dP - (s_L - s_G)\,dT \tag{10a}$$

(with obvious notation). In terms of magnetic susceptibilities and effective field B, the dependence of the pressure P on M at constant T is therefore given by :

$$P(B) - P(0) = \int_0^B \frac{dB'}{v_L - v_G} \times \times \int_0^{B'} dB''[\chi_L(B'') - \chi_G(B'')]\,. \tag{10b}$$

This relation shows that the crucial physical quantity which determines the shape of the equilibrium diagrams is the difference $\chi_L - \chi_G$ as a function of M (or B).

For an ideal non degenerate gas, the function χ is very simple :

$$\chi = (\mu_n)^2 \frac{1 - M^2}{kT}\,. \tag{11a}$$

This gives a good approximation of χ_G, except near the critical point where the gas is relatively dense. On the other hand, $\chi(M)$ is not known for the liquid phase and one has to resort to various approximations to calculate the M dependence (see for example the discussions in [3, 20-25]).

The pressure change for small values of M is easily evaluated expanding equation (10b) up to terms in B^2. One finds :

$$P(B) - P(0) = \frac{1}{2}\frac{1}{v_L - v_G}(\chi_L - \chi_G)\,B^2 \tag{11b}$$

where v and χ are the values at $B = 0$. Experimentally, one finds ([27-30])

$$\chi_L < \chi_G \tag{11c}$$

and, consequently, the curve $P(B)$ always has a parabolic behaviour with a positive curvature at the origin, as shown in the left part in figure 2b. Equation (11b) can be further simplified when one notices that at low temperatures $v_L \ll v_G$ and that the gas in equilibrium with the liquid is non degenerate ($Pv_G \simeq kT$). One can then write :

$$\frac{\Delta P}{P} = \frac{1}{2}\left(\frac{\mu_n B}{kT}\right)^2\left(1 - \frac{\chi_L}{\chi_G}\right) \tag{11d}$$

where we have used $\chi_G = \mu_n^2/kT$. Equation (11d) predicts $\Delta P/P = 0.9 \times 10^{-4}$ at $T = 0.5$ K and $\Delta P/P = 0.06 \times 10^{-4}$ at $T = 1$ K if a magnetic field of 20 T is applied to the system ($M_G \simeq 1.5\,\%$).

On the other hand, we know from the discussion of section 1.1 that the equilibrium pressure $P(M = 1)$ may in some cases be smaller than for $M = 0$. Because $\chi_L < \chi_G$ at $M = 0$, this implies a situation where, at fixed temperature ($T > T^*$), the equilibrium pressure first increases quadratically from P_0 as a function of M_L (or M_G), goes through a maximum $P = P_a$ at some intermediate value of the polarization $M = M_a$, and finally reaches a lower value P_1 when $M_L = M_G = 1$. In other words, when P decreases, the first contact between the two g curves occur at $M = M_a$, as shown in figure 3a ; when $P = P_a$ and $M = M_a$, the two g curves are tangent, which means that the effective magnetic fields of the two phases are equal.

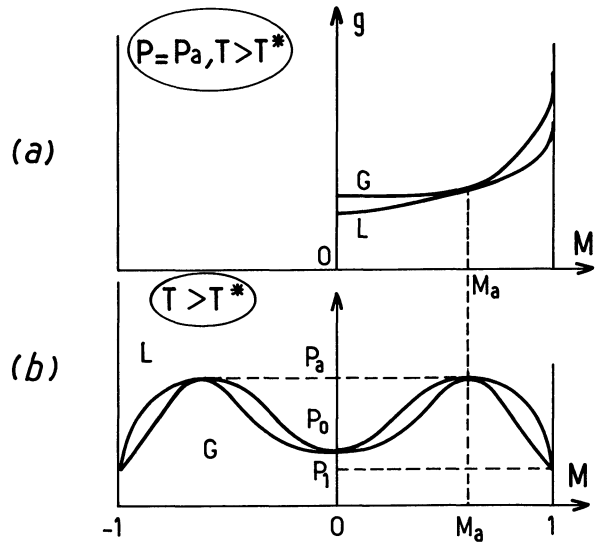

Fig. 3. — If $T > T^*$, that is if the saturating vapour pressure of the polarized liquid is smaller than that of the ordinary liquid, the phase diagram has the shape shown in figure (b) ; the pressures are increasing functions of M at low M's (because the magnetic susceptibility is smaller in the liquid than in the gas phase), go through an « azeotropic » maximum $P = P_a$ at $M = M_a$, and then decrease. Figure (a) shows the tangent contact between the two g curves when $P = P_a$. If P decreases from P_a, there are two common tangent to the g curves (until P reaches P_1).

The equilibrium curve therefore has the « moustache » shape shown in figure 3b, with three « azeotropic » points : in addition to the usual $M = 0$ point, two symmetrical azeotropic points correspond to particular values of the magnetization ($M = \pm M_a$) for which, as unpolarized ^{3}He, polarized liquid ^{3}He boils at fixed pressure (or fixed temperature if P is kept constant). Like around $M = 0$, the curvatures of the two curves are in the ratio of the magnetic susceptibilities, and the geometrical dispos-

(*) See [18, 19] for similar discussion in the context of solid-liquid equilibrium.

ition shows that, necessarily :

$$\chi_L(M_a) > \chi_G(M_a) \qquad (12)$$

in contrast with (11c) (both χ's nevertheless remain positive). This means that if, at low M, the magnetic susceptibility of the liquid is lower than that of the gas, it increases faster as a function of M and catches up χ_G at some value $M < M_a$. An important feature of these diagrams is that they imply unusual situations where the liquid nuclear polarization exceeds that of the gas.

Finally, we note that if $P\uparrow < P_0$ implies necessarily the existence of a polarized azeotropic point, the converse is not true : such non-zero M azeotropic points may also occur when $T < T^*$ (Fig. 4) and even be the general case.

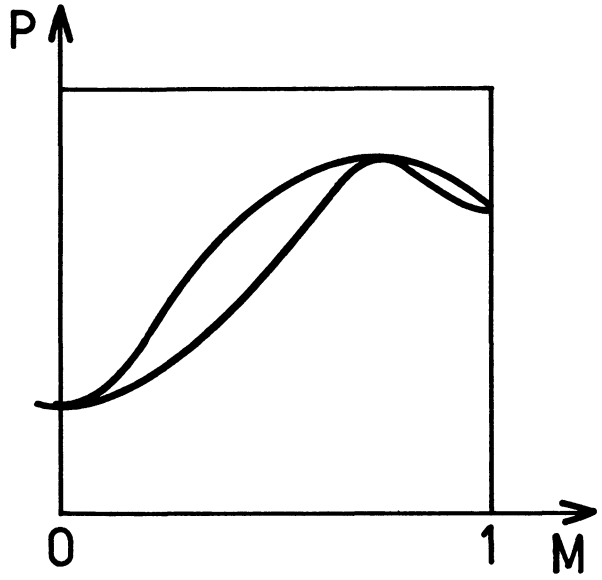

Fig. 4. — Another diagram with a non-zero M azeotropic point, but where $P\uparrow > P$ $(M = 0)$.

1.4 METAMAGNETISM. — We now consider a case where the g curve of the liquid phase has the shape shown in figure 5a : it has two inflexion points and a concave part. For magnetizations below $M = M_1$ or above $M = M_2$ (see Fig.), the system will behave as before, but for intermediate polarizations $(M_1 < M < M_2)$, it can reduce its Gibbs free energy by spontaneously separating into two phases of magnetizations M_1 and M_2. Then, the point representing the system lies on the common tangent AB shown in the figure (convex envelope).

Between points A and C, and between D and B, the system may remain in a metastable state, because it can only gain Gibbs energy by separating into two phases of completely different M. This is not true between C and D where a local instability occurs, so that this part of the curve is actually unphysical.

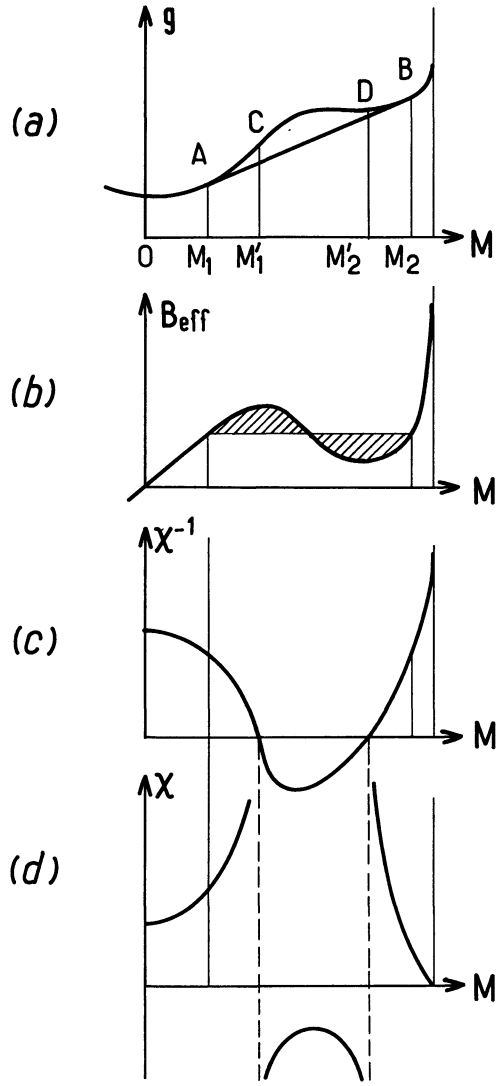

Fig. 5. — Gibbs energy curve for a homogeneous phase having a metamagnetic transition (Fig. (a)), corresponding effective field (Fig. (b)), and magnetic susceptibilities (Figs. c and d). The system remains homogeneous if $M < M_1$ or $M > M_2$, but spontaneously separates into two phases with different M's if $M_1 < M < M_2$; nevertheless, if $M_1 < M < M_1'$ or $M_2' < M < M_2$, the system can remain homogeneous in a metastable state. The magnetizations M_1 and M_2 can be obtained by a Maxwell construction on the curve giving the effective field B_{eff} as a function of M. They correspond to divergences of the magnetic susceptibility.

Curve (5b) shows the variations of the effective field. With this curve, a Maxwell construction gives the magnetizations M_1 and M_2 of the two phases. Curves (5c) and (5d) show $\chi^{-1}(M)$ and $\chi(M)$. Negative values of χ are unphysical, but χ can go (positively) to infinity on metastable branches when $M \underset{-}{\longrightarrow} M_1'$ or $M \underset{+}{\longrightarrow} M_2'$.

Following other authors [5, 19], we shall call *metamagnetism* this divergence of χ at finite B_{eff}, leading to spontaneous separation into two different

phases. The construction in figure 1a shows that μ_+ and μ_- are constant along the metamagnetic tangent AB. Also, whenever the system is stable (or metastable), one can show that :

$$\frac{\partial \mu_+}{\partial M} > 0 \quad \text{and} \quad \frac{\partial \mu_-}{\partial M} < 0 \qquad (13)$$

(at fixed P, T).

In the numerical model presented below, we find metamagnetic situations for some values of the parameters. For the moment, we only remark that, the smaller χ_L and the smaller ΔE (Eq. (5a)), the more likely metamagnetism is : this is because g then starts at small M's with a strong curvature but ends up at a low value for $M = 1$, which favours the occurrence of a convex part at intermediate values of M.

1.5 COMBINATION OF TWO INSTABILITIES. — We finally discuss how the two instabilities in the liquid (vaporization when the pressure is decreased, and metamagnetism when M changes) combine in phase diagrams. The situation is similar to that of paragraph 1.2 and paragraph 1.3, except that the g diagram for the liquid now has a straight line portion.

If we add metamagnetism to the diagram in figure 2, when P decreases, a situation such that shown in figure 6a will occur : at some value of P, the common tangent to both g curves will be the line AB which is tangent to g_L in two points, A and B. For slightly higher values of the pressure, the contact point of the common tangent will be close to B ; but, for slightly smaller values of P, it jumps to A, with a different value of M. Hence, the diagram shown in figure 6b, with a plateau A' B' on the liquid curve, and a reentrant kink point E' on the gas curve. Metastable situations (with respect to liquid metamagnetic separation) can occur when the contact point does not jump to the other bump of the curve. This is possible until the point reaches point C (or D), where the g curves become unphysical. Such metastable situations correspond to the dashed curves in figure 6b. The dotted-dashed lines are the border of the domain where the metamagnetic phase separation occurs in the liquid.

If we add metamagnetism in figure 3, two main cases are possible : either M_a falls outside of the metamagnetic range of the liquid phase, or it falls inside so that the first tangent contact of the two g curves shown in figure 3a now occurs in a point where g_L is a straight line. The first possibility is shown in figure 7a (moustache with plateaus), the second in figure 7b (a curve that we nicknamed « diavolo »). In figure 7, we have assumed the metamagnetic effect in the liquid phase to disappear at high pressure, but this is not necessarily the case :

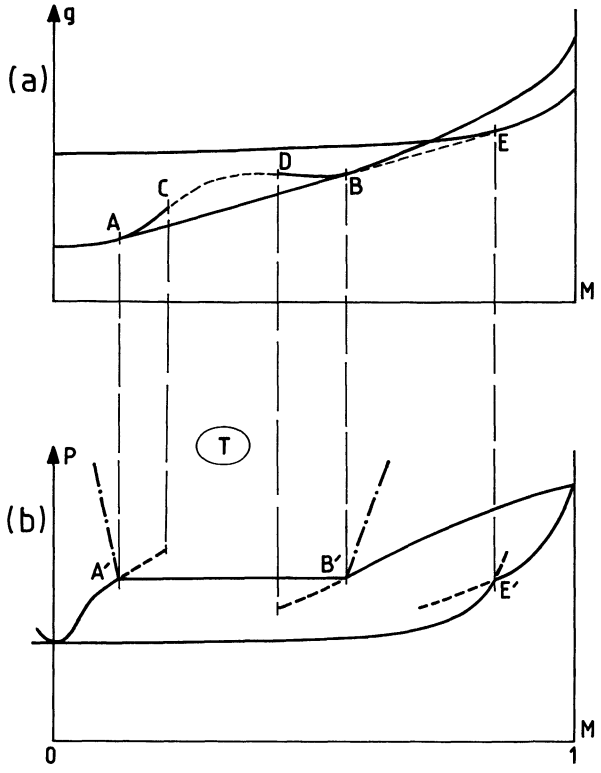

Fig. 6. — Liquid-gas equilibrium curves when the liquid can be metamagnetic. Points A and B on the g_L curve correspond on the equilibrium curves to a plateau A' B' and a kink at point E'. The dotted dashed lines in figure (b) show the metamagnetic diagram of the liquid phase (in the absence of gas). Dashed lines in figure 6b correspond to metastable situations where the liquid remains homogeneous, but could decrease its Gibbs free energy by undergoing a metamagnetic transition. The end of these dashed lines occurs at a pressure where the curve g_G becomes tangent to the common tangent in C and D of the curve g_L.

the metamagnetic separation line (dashed curve) does not always close at the top, as we will see in section 3. Moreover, other more complicated situations are of course possible (more azeotropic points or metamagnetic plateaus). A general discussion of equilibrium diagrams and singular points, in the case of phase changes of mixtures of two substances, can be found in Landau and Lifschitz [31] and transposed to polarized ^{3}He (M being analogous to concentration).

2. Formalism.

In the preceding section, the thermodynamic potential used was the Gibbs free energy ; this is well adapted to a discussion of equilibrium between phases at the same temperature and pressure, but with different molar volumes. In this section, where we wish to treat phenomenologically the interactions between particles, it is much more convenient to use

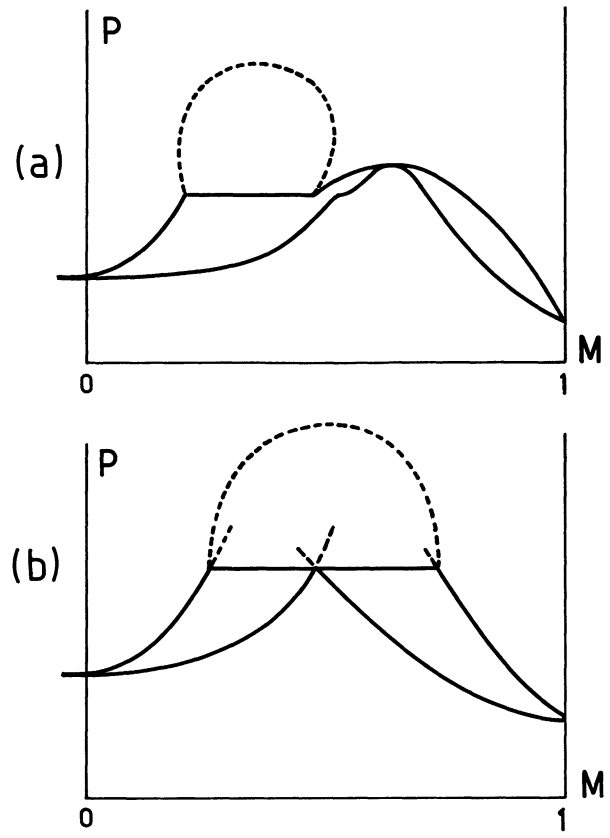

Fig. 7. — Two other diagrams combining metamagnetism and evaporation.

the volume (that is the density) as a thermodynamical variable, and the Helmholtz free-energy F as a potential.

2.1 HELMHOLTZ FREE-ENERGY : MODELIZATION OF THE INTERACTION TERM. — The variables we now take are M, T, and the total number density ρ :

$$\rho = N/V \tag{14a}$$

(N : number of particles, V : volume). If $\rho\uparrow$ and $\rho\downarrow$ are the partial number densities, one obviously has

$$\rho\uparrow + \rho\downarrow = \rho$$
$$M = \frac{\rho\uparrow - \rho\downarrow}{\rho} \tag{14b}$$

where M is the relative (dimensionless) magnetization. Rather than F, we shall use the free-energy f per unit volume (*) :

$$f = F/V \tag{15a}$$

(*) Here, a lower case letter corresponds to a thermodynamical function per unit volume, and not per atom as in section 1.

and assume that :

$$f(\rho, M, T) = f_{ni}(\rho, M, T) + f_v(\rho, M, T). \tag{16}$$

In this expression, f_{ni} is the free energy density of a non-interacting Fermi gas [32], which can be written :

$$f_{ni}(\rho, M, T) = f_{ni}(\rho\uparrow, T) + f_{ni}(\rho\uparrow, T)$$

while f_v is the contribution to f due to the interactions. Obviously, this function can not be calculated exactly and we use here a phenomenological model to obtain its value. Actually, we simply generalize the expression used in BPS (for unpolarized ^{3}He) to non-zero M values, and write the expression :

$$f_v = \frac{1}{2}[b_0 + b_1 M^2 + b_2 M^4]\rho^2 + \frac{1}{2}[c_0 + c_1 M^2 + c_2 M^4]\rho^{2+\sigma} \tag{17}$$

which includes explicitly a M dependence up to terms in M^4. In BPS, parameters b_0 and c_0 were chosen in order to reproduce the experimental values of the energy per particle, the density and the incompressibility of unpolarized liquid ^{3}He at zero pressure and $T = 0$. The resulting predictions for the liquid-gas phase transition were in reasonable agreement with the experimental data ; in particular the vapour pressure was reproduced within 20 % at all temperatures of equilibrium. Nevertheless, in the present work, we are interested in finer details than in BPS, and we shall follow a different strategy to fix the values of the parameters in (17), and actually take some of them temperature dependent.

The values of b_0, c_0 and σ we take at $T = 0$ are those of BPS. For simplicity, we assume that c_0 and σ do not depend on T($c_0 = 871.487 \times 10^4$ K Å$^{3(1+\sigma)}$, $\sigma = 2.658$) but, for b_0, we include a T dependence which is fixed in order to reproduce exactly at each temperature the experimental values of the saturating vapour pressure of unpolarized ^{3}He [33]. Table I shows that b_0 then depends only weakly on T, as could be expected from the quality of the result obtained in BPS for the saturating pressure.

We have seen in section 1 that the magnetic susceptibility χ plays a crucial role in the problem studied here. We therefore wish to reproduce precisely the corresponding experimental values. Within the frame of our model, the value of χ is given by

$$(\mu_n)^2 \chi^{-1} = \frac{1}{N}\left(\frac{\partial^2 F}{\partial M^2}\right)_{p,T} = \frac{1}{\rho}\left(\frac{\partial^2 f}{\partial M^2}\right)_{p,T}$$
$$= (\mu_n)^2 (\chi_{ni})^{-1} + (b_1 + 6\, b_2 M^2)\rho + (c_1 + 6\, c_2 M^2)\rho^{1+\sigma} \tag{18}$$

Table I. — *Values of the free energy parameters as a function of T.*

T (K)	b_0 (K Å^3)	b_1 (K Å^3)	c_1 (K Å$^{3(1+\sigma)}$)
0.2	− 824.69	− 183.25	3.5814 × 10^5
0.25	− 826.37	− 181.12	3.3658 × —
0.3	− 828.15	− 179.46	3.3757 × —
0.35	− 829.97	− 177.48	3.3252 × —
0.4	− 831.80	− 174.45	2.8087 × —
0.45	− 833.66	− 171.98	2.5798 × —
0.5	− 835.34	− 170.36	2.7346 × —
0.55	− 837.02	− 168.30	2.7188 × —
0.6	− 838.62	− 166.07	2.6305 × —
0.65	− 840.13	− 163.97	2.6070 × —
0.7	− 841.55	− 161.65	2.4818 × —
0.8	− 844.08	− 156.88	2.1653 × —
0.9	− 846.18	− 152.60	1.9806 × —
1	− 847.82	− 148.06	1.6401 × —
1.2	− 849.67	− 140.33	1.2974 × —
1.4	− 849.57	− 133.57	1.0933 × —
1.8	− 843.77	− 121.71	0.6308 × —

where χ_{ni} is the magnetic susceptibility of the polarized non interacting Fermi gas. The parameters b_1 and c_1 are consequently chosen in order to reproduce the experimental values of $\chi(T)$ [34] for two different values of ρ, 33.0 and 35.5 cm^3/mole. We have checked that our fit is able to accurately reproduce $\chi(T)$ up to $\rho = 32.0$ cm^3/mole, which is well above the values which appear in our calculations. The values of $b_1(T)$ and $c_1(T)$ are also shown in table I.

In order to fix the value of the remaining two parameters b_2 and c_2, we have considered equations (16) and (17) for the fully polarized system ($M = 1$)

$$f\uparrow(\rho, T) = f_{ni}\uparrow(\rho, T) + \frac{1}{2} b\uparrow \rho^2 + \frac{1}{2} c\uparrow \rho^{2+\sigma} \tag{19}$$

where

$$b\uparrow = b_0 + b_1 + b_2 \; ; \quad c\uparrow = c_0 + c_1 + c_2 \, .$$

Since we chose T dependent parameters for the unpolarized phase, we could in the same way assume that $b\uparrow$ and $c\uparrow$ depend on T. Nevertheless, for the fully polarized phase, no experimental data are yet available, which could be used to fit the parameters. Then, we shall simply assume that $b\uparrow$ and $c\uparrow$ are T independent. This absence of temperature dependence of the parameters of the fully polarized phase is actually not sufficient to fix them univoquely : they will be fixed by assuming given values for the binding energy $E\uparrow$ and the saturation density $\rho_0\uparrow$ of the polarized liquid at $T = 0$. Both $E\uparrow$ and $\rho_0\uparrow$ then appear as the natural free parameters of our model.

It is important to realize that, in our calculations, the non interacting parts of equations (16) and (19) are computed exactly, by calculating the Fermi integrals that enter their definitions [35]. This is crucial since we wish to describe a wide spectrum of situations ranging from the classical regime in the gas (low density) to the degenerate limit in the liquid (high density).

2.2 PHASE TRANSITIONS. — Simple as it might seem, the free energy functional of equation (16) is of great richness. We now show how it allows the study of coexistence between different phases.

Homogeneous partially polarized ^{3}He is not necessarily stable for all values of ρ, M and T, due to combined effects of statistics and interactions. Necessary conditions for the stability of a binary system made of spin up and spin down atoms, are [36] :

$$c_V = \left(\frac{\partial u}{\partial T}\right)_{\rho, M} \geqslant 0 \tag{20a}$$

$$\kappa = \left(\frac{\partial P}{\partial \rho}\right)_{T, M} \geqslant 0 \tag{20b}$$

$$\left(\frac{\partial \mu_+}{\partial M}\right)_{P, T} \geqslant 0 \quad \text{or} \quad \left(\frac{\partial \mu_-}{\partial M}\right)_{P, T} \leqslant 0 \tag{20c}$$

where u is the internal energy *per* unit volume

$$u = f - T\left(\frac{\partial f}{\partial T}\right)_{\rho, M} \tag{21}$$

κ the compressibility (μ_+ and μ_- are the chemical potentials defined in Sect. 1). The value of the pressure P and of the μ's are given by

$$P(\rho, M, T) = \rho^2 \left[\frac{\partial}{\partial \rho}\left(\frac{f}{\rho}\right)\right]_{T, M} =$$

$$= P_{ni}(\rho, M, T) + \frac{1}{2}\left[b_0 + b_1 M^2 + b_2 M^4\right]\rho^2 + \frac{1}{2}(1+\sigma)\left[c_0 + c_1 M^2 + c_2 M^4\right]\rho^{2+\sigma} \tag{22}$$

and :

$$\mu_{+,-}(\rho, M, T) = \mu^{ni}_{+,-}(\rho\uparrow, \downarrow ; T) + \frac{\partial f_V(\rho, M, T)}{\partial \rho\uparrow, \downarrow} \tag{23}$$

where $\mu^{ni}_{+,-}$ is the chemical potential of an ideal Fermi gas. It is straightforward to evaluate the contributions of the interactions to $\mu_{+,-}$, because :

$$\frac{\partial f_V}{\partial \rho \uparrow, \downarrow} = \frac{\partial f_V}{\partial \rho} + \frac{\partial f_V}{\partial M} \frac{\partial M}{\partial \rho \uparrow, \downarrow} \quad (24a)$$

with

$$\frac{\partial M}{\partial \rho \uparrow, \downarrow} = \pm 2 \frac{\rho \downarrow, \uparrow}{\rho^2} . \quad (24b)$$

In addition to conditions (20), the pressure P must be positive.

In general, a violation of the stability criteria (20) indicates the occurrence of a phase separation : the system splits into separate phases in equilibrium. The phases can differ in ρ and/or M. It is important however to stress that these conditions are necessary but not sufficient for stability (they can be satisfied in regions where the system is not stable, but only metastable, as discussed in Sect. 1). We have verified that condition (20a) for the specific heat is satisfied for all the values of ρ and T encountered in our calculation. Conversely, situations have been frequently found where conditions (20b) and (20c) are violated. In particular, at low temperatures condition (20b) is violated in a wide range of values of ρ for M fixed. This region of negative compressibility is associated with a liquid-gas phase transition and was already found in BPS for unpolarized ^{3}He ($M = 0$). The properties of such a phase transition will be explicitly illustrated in the next section for the fully polarized case ($M = 1$). Values of M at which condition (20c) is violated have also been frequently met at high density (liquid) and low temperatures. Condition (20c) is equivalent to requiring that $\chi > 0$; its violation is responsible for the phenomenon of metamagnetism (see Sect. 1).

To find two phases in equilibrium we have to solve the system of equations :

$$\begin{aligned} P(\rho_1, M_1, T) &= P(\rho_2, M_2, T) \\ \mu_{+,-}(\rho_1, M_1, T) &= \mu_{+,-}(\rho_2, M_2, T) . \end{aligned} \quad (25)$$

In principle the Gibbs phase rule would allow for the equilibrium of three or even four phases. Actually, in our calculation we have found only three phases in equilibrium at most. This corresponds to two liquids characterized by rather close values of ρ but significantly different values of M, in equilibrium with a gas.

3. Results.

In this section we present the results for the phase diagrams predicted by the phenomenological model described in the previous section. The free parameters of the model are the binding energy $E\uparrow$ and the $T = 0$ saturation density $\rho\uparrow$ of the fully polarized system. The values of $E\uparrow$ and $\rho\uparrow$ are not presently known, although from theoretical arguments (confirmed by recent microscopic calculations [22, 37]) one expects that they should not differ very much from the corresponding values in the unpolarized phase

$$(E = -2.5 \text{ K}, \ \rho_0 = 0.0165 \text{ atom } /\text{Å}^3) .$$

We have first assumed $\rho_0\uparrow = \rho_0$ and made two different choices for $E\uparrow$: $E\uparrow = -2.4$ K and $E\uparrow = -2.2$ K. The former choice corresponds to an energy gap $\Delta E = E\uparrow - E = 0.1$ K which is smaller than that ($\Delta E \simeq 0.18$ K) obtained extrapolating to $M = 1$ the low M behaviour of the energy at $T = 0$:

$$E(M) = E + \frac{1}{2} \frac{\mu_n^2}{\chi} M^2 . \quad (25)$$

This choice is then a natural candidate to provide the phenomenon of metamagnetism. Conversely, with the latter choice one does not expect to find metamagnetism at low pressures. The values of the parameters $b\uparrow$ and $c\uparrow$ (see Eq. (19)) corresponding to the two choices are shown in table II. With these choices for $b\uparrow$ and $c\uparrow$, the free energy of the system (Eqs. (16) and (17)) is completely determined as a function of ρ, M and T.

We have first explored the fully polarized system ($M = 1$). In this case we find the typical phase diagrams in figure 8 characterizing the liquid gas phase transition. A critical temperature $T_c\uparrow = 5.36$ K is found with the choice $E\uparrow = -2.4$ K, $\rho_0\uparrow = \rho_0$. This value is higher than the one found in BPS for unpolarized ^{3}He ($T_c = 4.32$ K). Of course, the absolute values should not be taken too seriously, since in the unpolarized phase the present method overestimates the critical temperature by $\simeq 30$ %. The relative increase of $T_c\uparrow$ with respect to T_c is however in reasonable agreement with the estimate of [8] based on the theory of corresponding states improved to account for the effects of statistics [38].

Table II.

	$b\uparrow$	$c\uparrow$
$E\uparrow = -2.4$ K	$-1\,046.77$ K Å^3	993.53×10^4 K Å$^{3(1+\cdot)}$
$E\uparrow = -2.2$ K	$-1\,013.41$ K Å^3	943.61×10^4 K Å$^{3(1+\sigma)}$

Let us now discuss the results for the partially polarized system. As seen in the previous sections, a key quantity, which characterizes the structure of the liquid-gas phase transition as well as of the possible metamagnetic transition, is the magnetic susceptibility χ. In figure 9a and b we plot $\mu_n^{-2}\chi$ as a function of M for a value of the density which is typical of the liquid phase and for two different

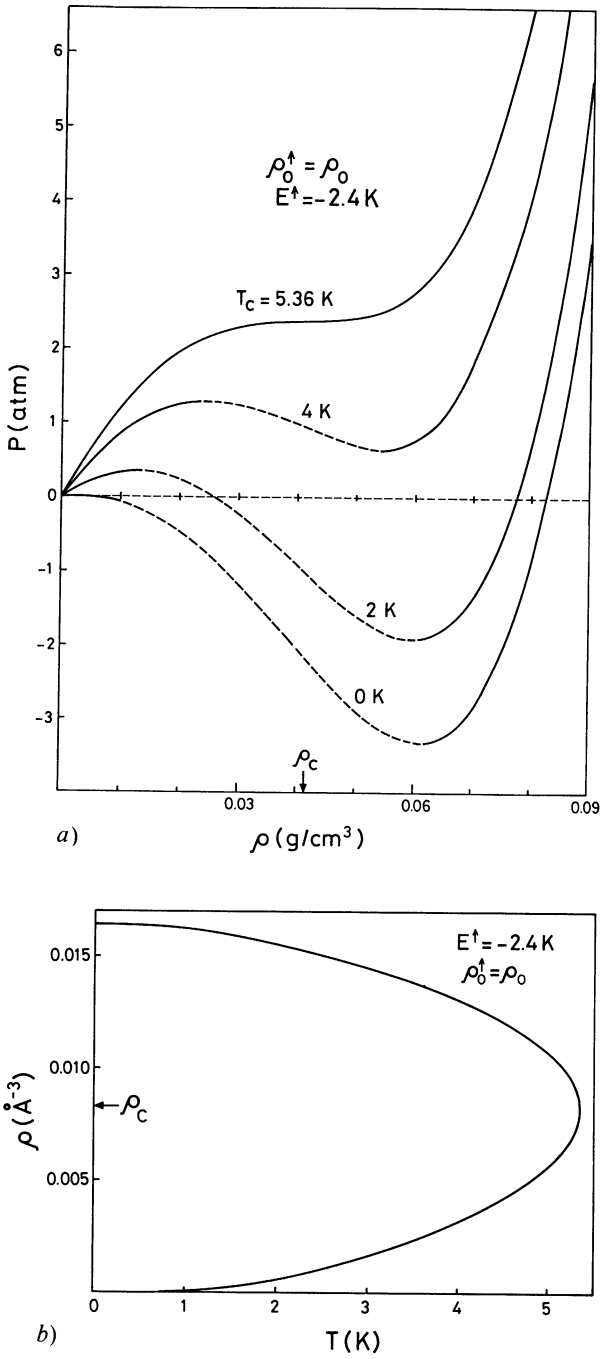

Fig. 8. — a) Equation of state diagrams predicted for fully polarized ^{3}He. The obtained critical temperature is $T_c = 5.36$ K. b) Temperature dependence of the densities of the two phases in equilibrium (liquid and gas).

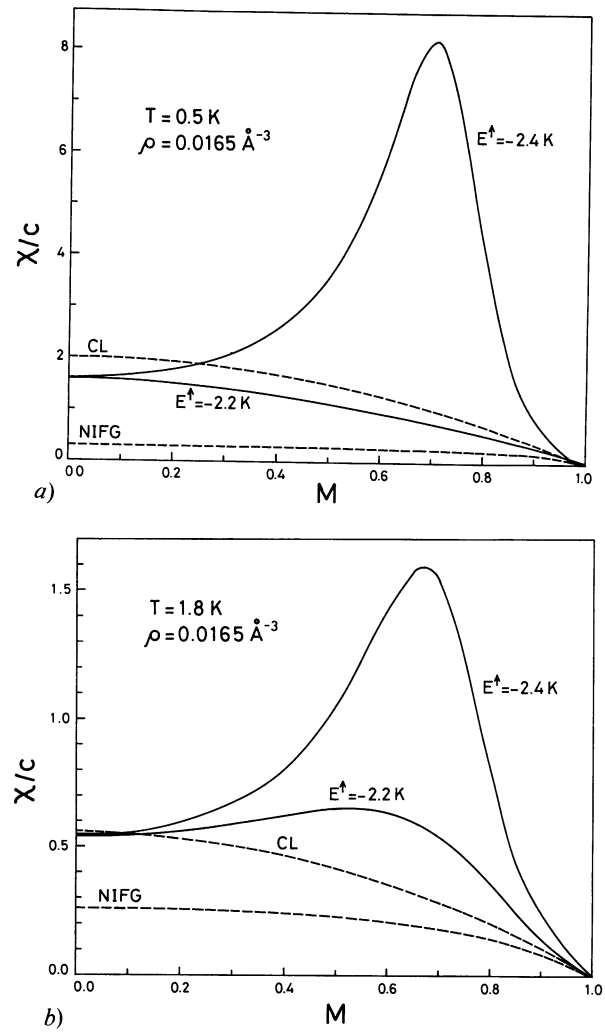

Fig. 9. — Magnetic susceptibilities χ/c (with $c = \mu_n^2$) of the liquid phase of ^{3}He, at fixed temperature, as a function of the relative magnetization M. Two different values of the free parameter $E\uparrow$ are taken (– 2.2 and – 2.4 K), but $\rho_0\uparrow$ is kept fixed and equal to ρ_0. As a point of comparison, the magnetic susceptibilities of a classical gas (CL) and a non interacting Fermi gas (NIFG) are also shown.

temperatures. In the figures we also show the susceptibility of the classical non interacting gas (CL) (see Eq. (11a)) which very accurately describes the behaviour of the gas in equilibrium with the liquid. We also show, for comparison, the prediction of the non interacting Fermi gas (NIFG). We notice that at small M, χ is always smaller than χ_{CL}. However, depending on the assumption on $E\uparrow$ and on the value of T, χ can become larger than χ_{CL} when M increases. As discussed in section 1.3, this behaviour is consistent with the existence of a maximum value for the vapour pressure at some intermediate value of M. The figures 9 do not exhibit the metamagnetic effect (negative χ) because they correspond to relatively high values of T.

Figures 10 show the phase diagram obtained with $E\uparrow = -2.2$ K and $\rho_0\uparrow = \rho_0$. As expected, we do not find metamagnetism in this case (we have not, however, explored the very low temperature regime). The occurrence of the cross-over temperature predicted in section 1.1 emerges in a clear way, though it occurs at a higher value ($T \simeq 0.9$ K) than predicted by equation (5b) ($T^* = 0.45$ K). One should however remark that at such temperatures

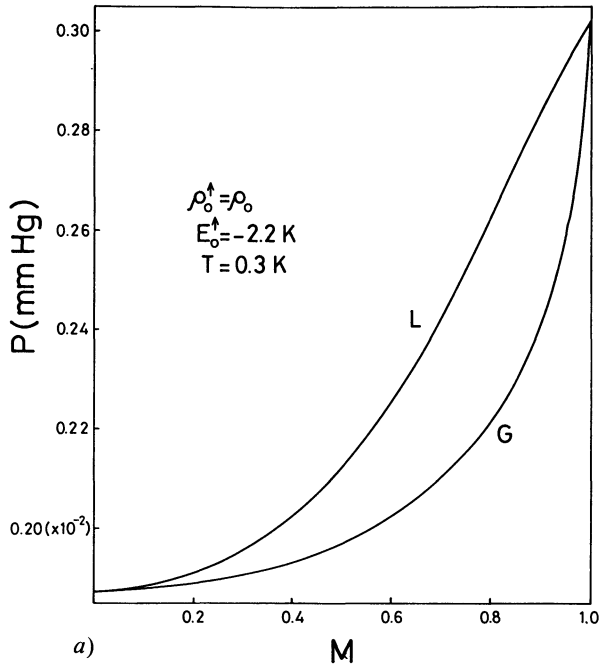

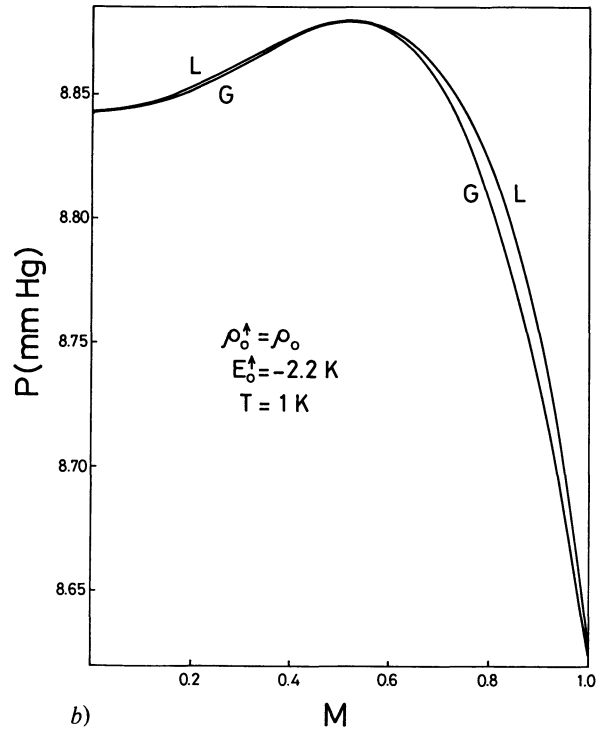

Fig. 10. — Phase diagrams of liquid-gas equilibrium for partially polarized ^{3}He at three different (fixed) temperatures. The free parameters are fixed at the values $E\uparrow = -2.2$ K and $\rho_0\uparrow = \rho_0$. The cross-over temperature is $T^* \simeq 0.9$ K.

the effects of non degeneracy in the liquid, neglected in equation (5b), can be rather important.

Figures 11a, b and c show the results obtained with choice $E\uparrow = -2.4$ K and $\rho_0\uparrow = \rho_0$. In this case, indeed, we find metamagnetism when $T \lesssim 0.4$ K. The effect is very spectacular at $T = 0.2$ K

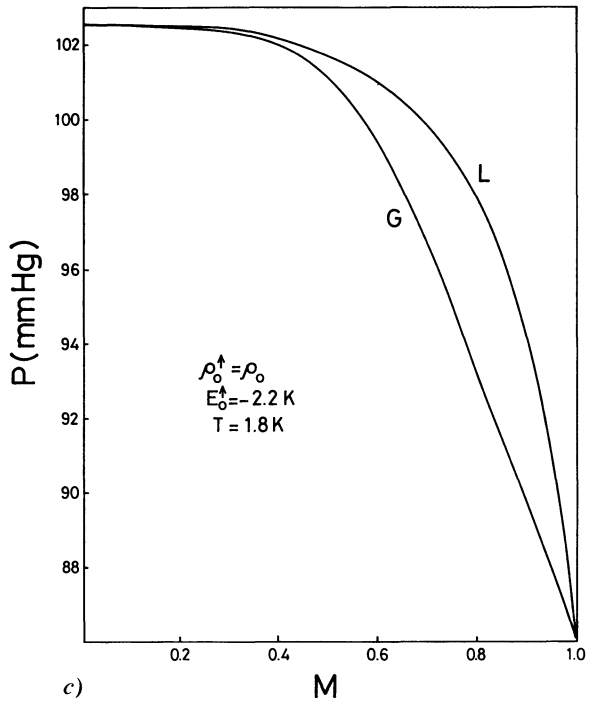

(Fig. 11a) where we find the « diavolo » predicted in section 1.5. At $T = 0.35$ K we find another situation (Fig. 11b) already anticipated in section 1.5 (moustache with plateau). The curves of metastability (with respect to the metamagnetic separation) are also drawn. The cross-over temperature is found to occur at $T^* < 0.2$ K consistently with the prediction of equation (5b) ($T^* = 0.14$ K).

We finally discuss the role of the parameter $\rho_0\uparrow$. By varying this parameter by $-5\,\%$ with respect to ρ_0 we have found that the liquid gas phase transition are only weakly modified. Conversely by taking $\rho\uparrow = 1.05\,\rho_0$ we have found some modification in the liquid metamagnetism. In this case the metamagnetic separation line does not close at high pressures (see Fig. 12), in opposition to the case $\rho_0\uparrow = \rho_0$ and $\rho_0\uparrow = 0.95\,\rho_0$.

Conclusion.

The phenomenological model used in this article gives interesting predictions in several cases, and shows that the binding energy of the fully polarized phase plays a crucial role in determining the polarized liquid-gas equilibrium curves of partially polarized ^{3}He. Even if this binding energy were known precisely, which might be the case with the impressive progress made in recent variational calculations [37], one should keep in mind that our model remains phenomenological : it is based on assumption that equation (17) gives a good approximation of the effects of interaction on the free energy of the system. Such a simple M^2 and M^4 interpolation is

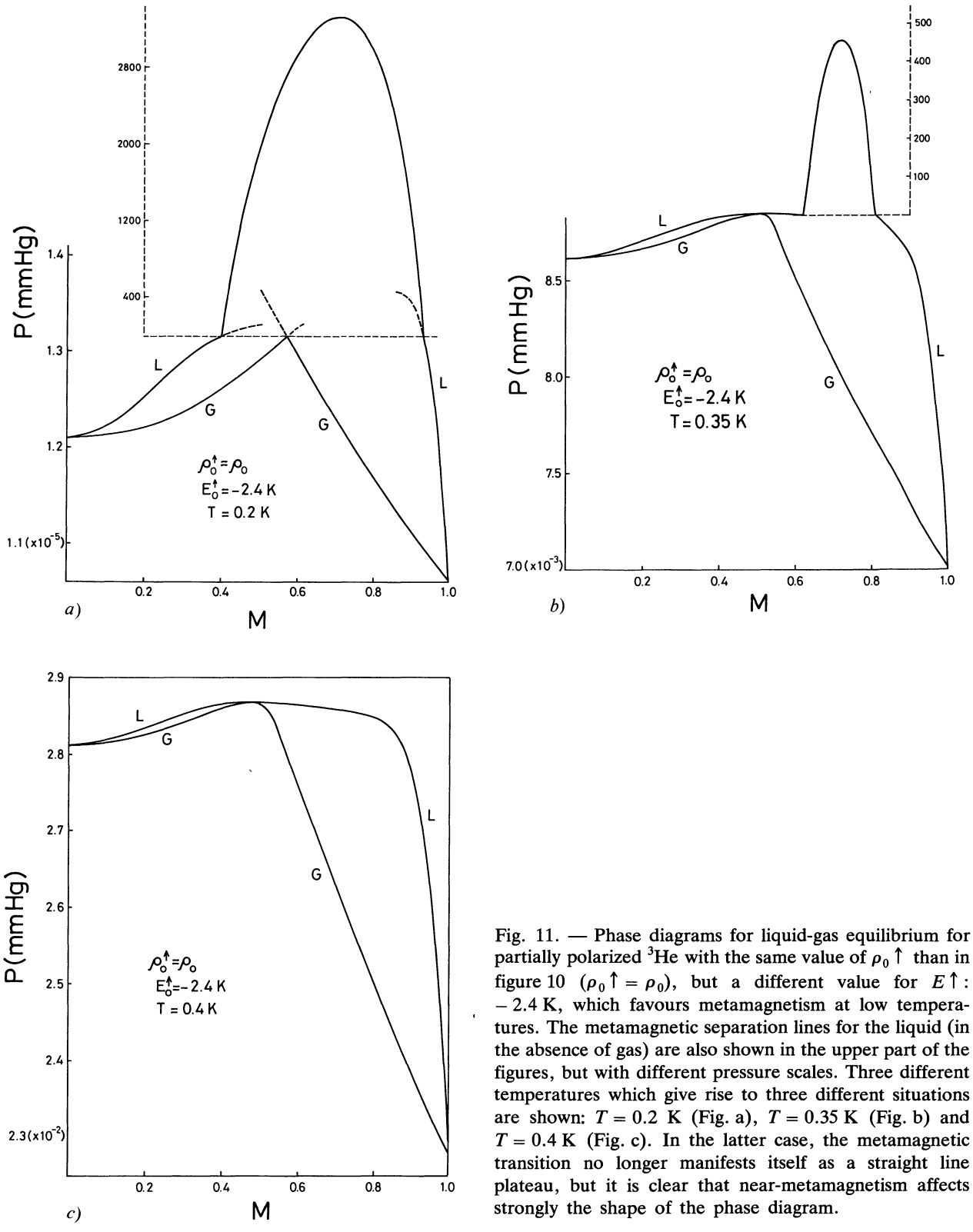

Fig. 11. — Phase diagrams for liquid-gas equilibrium for partially polarized ^{3}He with the same value of $\rho_0\uparrow$ than in figure 10 ($\rho_0\uparrow = \rho_0$), but a different value for $E\uparrow$: − 2.4 K, which favours metamagnetism at low temperatures. The metamagnetic separation lines for the liquid (in the absence of gas) are also shown in the upper part of the figures, but with different pressure scales. Three different temperatures which give rise to three different situations are shown: $T = 0.2$ K (Fig. a), $T = 0.35$ K (Fig. b) and $T = 0.4$ K (Fig. c). In the latter case, the metamagnetic transition no longer manifests itself as a straight line plateau, but it is clear that near-metamagnetism affects strongly the shape of the phase diagram.

indeed plausible, but not certain. It has the merit of being the simplest model able to include non trivial effects such as metamagnetism. Adding higher order corrections could of course change quantitatively the predictions of the model for large polarizations. Nevertheless, as long as the general shape of the curves is not changed (in particular, the number of inflexion points in Fig. 5a), the general conclusions that we have obtained remain qualitatively valid.

If the $M^2 - M^4$ interpolation turns out to be a good approximation, our predictions could be useful for future experiments. Several of the diagrams

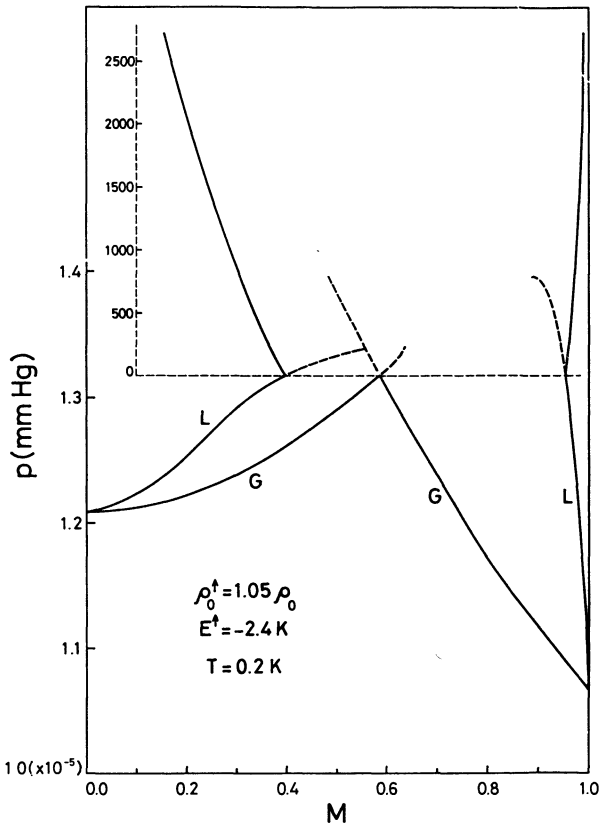

show that most of the interesting effects occur only beyond $M = 50\,\%$, a valuable information. Moreover, even if metamagnetism does not occur, figure 11c shows how « near metamagnetism » could play an important role, as pointed out in [5]. One could imagine purely thermal overpolarization methods taking advantage of the particular shape of these diagrams.

Note added in proof: phase diagrams corresponding to $E_0\uparrow = -2.3$ K can be found in Ref. [39].

Acknowledgments.

This work was supported in part by CAICYT (Spain) grant PB 85-0072-C02-00. Two authors (P. J. N. and F. L.) belong to the « Laboratoire Associé n° 18 au CNRS ».

Two authors (M. B. and S. S.) wish to thank the Orsay IPN Institute for hospitality when this work was started. We also thank the DPh-N/MF Service at Saclay where parts of the calculation were performed.

◀

Fig. 12. — Same figure as figure 11a, but with a larger value for the density $\rho_0\uparrow$. The metamagnetic separation line no longer closes at high pressures.

References

[1] DUTTA, A. and ARCHIE, C. N., *Phys. Rev. Lett.* **55** (1985) 2949.

[2] BONFAIT, G., PUECH, L., GREENBERG, A. S., ESKA, G., CASTAING, B. and THOULOUZE, D., *Phys. Rev. Lett.* **53** (1984) 1092.

[3] CASTAING, B. and NOZIÈRES, P., *J. Physique* **40** (1979) 257.

[4] CASTAING, B., communication at the 1984 Gordon Conference on Spin Polarized Quantum System. See also [19].

[5] BEDELL, K. S. and SANCHEZ-CASTRO, C., *Phys. Rev. Lett.* **57** (1986) 854.

[6] FROSSATI, G., BEDELL, K. S., WIEGERS, S. A. J. and VERMEULEN, G. A., *Phys. Rev. Lett.* **57** (1986) 1032.

[7] NACHER, P. J., LEDUC, M., TRÉNEC, G. et LALOË, F., *J. Physique Lett.* **43** (1982) L 525.

[8] LHUILLIER, C. et LALOË, F., *J. Physique* **40** (1979) 239.

[9] TASTEVIN, G., NACHER, P. J., WIESENFELD, L., LEDUC, M., and LALOË, F., in preparation.

[10] BARRANCO, M. and BUCHLER, J. R., *Phys. Rev.* **C 22** (1980) 1729.

[11] PI, M., VIÑAS, X., BARRANCO, M., PEREZ-CANYELLAS, A. and POLLS, A., *Astron. Astrophys., Suppl. Ser.* **64** (1986) 439 and references therein.

[12] SKYRME, T. H. R., *Philos. Mag.* **1** (1956) 1043 ; *Nucl. Phys.* **9** (1959) 615.

[13] VAUTHERIN, D. and BRINK, D. M., *Phys. Rev.* **C 5** (1972) 626.

[14] STRINGARI, S., *Phys. Lett.* **106A** (1984) 267, *Europhys. Lett.* **2** (1986) 639.

[15] BARRANCO, M., POLLS, A. and STRINGARI, S., *J. Physique* **48** (1987) 911.

[16] BEAL, B. T. and HATTON, J., *Phys. Rev.* **139A** (1965) 1751.

[17] LEFEVRE-SEGUIN, V., NACHER, P. J., BROSSEL, J., HARDY, W. N. et LALOË, F., *J. Physique* **46** (1985) 179.

[18] BONFAIT, G., CASTAING, B., SCHUHL, A. and CHAPELLIER, M., *J. Physique Lett.* **46** (1985) 1073.

[19] BONFAIT, G., PUECH, L., CASTAING, B. and THOULOUZE, D., *Europhysics Lett.* **1** (1986) 521.

[20] KROTSCHEK, E., CLARK, J. W. and JACKSON, A. D., *Phys. Rev.* **28B** (1983) 5088.

[21] GLYDE, H. R. and HERNADI, S. I., *Phys. Rev.* **29B** (1984) 3873.

[22] MANOUSAKIS, E., FANTONI, S., PANDHARIPANDE, V. R. and USMANI, Q. N., *Phys. Rev.* **28B** (1983) 3770.

[23] BEDELL, K. S., *Phys. Rev. Lett.* **54** (1985) 1400.

[24] BEAL-MONOD, M. T. and DANIEL, E., *Phys. Rev.* **B 27** (1983) 4467.

[25] VOLLHARDT, D., *Rev. Mod. Phys.* **56** (1984) 99.

[26] TAI KAI NG and SINGWI, K. S., *Phys. Rev. Lett.* **57** (1986) 226.

[27] FAIRBANK, W. M., ARD, W. B. and WALTERS, G. K., *Phys. Rev.* **95** (1954) 566.

[28] ABEL, W. R., ANDERSON, A. C., BLACK, W. C. and WHEATLEY, J. C., *Physics* **1** (1965) 337.
[29] KELLER, W. E., *Helium 3 and Helium 4* (Plenum Press) Chap. VI.
[30] RAMM, H., PEDRONI, P., THOMPSON, J. R. and MEYER, H., *J. Low. Temp. Phys.* **2** (1970) 539.
[31] LANDAU, L. et LIFSCHITZ, E., *Physique Statistique* (Editions Mir, Moscou), sections (97-102).
[32] PATHRIA, R. K., *Statistical Mechanics* (Pergamon Press) 1972.
[33] ROBERTS, T. R., SHERMAN, R. H., SYDORIAK, S. G., BRICKWEDDE, F. G., *Prog. Low Temp. Phys.* **4** (1964) 480.
[34] RAMM, H., *et al.*, *J. Low Temp. Phys.* **2** (1970) 539.
[35] BARRANCO, M. and TREINER, J., *Nucl. Phys.* **A 351** (1981) 269.
[36] LANDAU, L. and LIFSCHITZ, E. M., *Physique Statistique* (Editions Mir, Moscou) 1967.
[37] BOUCHAUD, J. P. and LHUILLIER, C., submitted to *Europhysics Lett.* **3** (1987) 1273.
[38] MILLER, M. D. and NOSANOV, L. H., *Phys. Rev.* **B 15** (1977) 4376.
[39] BARRANCO, M., POLLS, A., STRINGARI, S., NACHER, P. J., and LALOË, F., *J. Physique Colloq.* **48** (1987) C2-101.